Channels 5:1, 34-42; January/February 2011; © 2011 Landes Bioscience

Analyses of gating thermodynamics and effects of deletions in the mechanosensitive channel TREK-1

Comparisons with structural models

Grigory Maksaev,[1] Adina Milac,[2,3] Andriy Anishkin,[1] H. Robert Guy[2] and Sergei Sukharev[1,*]

[1]Department of Biology; University of Maryland; [2]Laboratory of Cell Biology; Center for Cancer Research; National Cancer Institute; National Institutes of Health; Bethesda, MD USA; [3]Institute of Biochemistry of the Romanian Academy; Bucharest, Romania

Key words: membrane tension, gating transition, channel domains, protein expansion

TREK-1, a mechanosensitive K channel from the two-pore family (K_2P), is involved in protective regulation of the resting potential in CNS neurons and other tissues. The structure of TREK-1 and the basis of its sensitivity to stretch and variety of lipid-soluble factors remain unknown. Using existing K channel structures as modeling templates, TREK-1 was envisioned as a two-fold symmetrical complex with the gate formed primarily by the centrally positioned TM2b helices of the second homologous repeat. Opening was modeled as a conical expansion of the barrel separating TM2b's accompanied by extension of TM2a helices with the cytoplasmic TM2a-TM1b connector. Seeking first experimental support to the models we have accomplished thermodynamic analysis of mouse TREK-1 gating and functional testing of several deletion mutants. The predicted increase of the channel in-plane area (ΔA) of ~5 nm^2 in models was supported by the experimental ΔA of ~4 nm^2 derived from the slope of open probability versus membrane tension in HEK-293T cells and their cytoskeleton-depleted blebs. In response to steps of suction, wild-type channel produced transient currents in cell-attached patches and mostly sustained currents upon patch excision. TREK-1 motifs not present in canonical K channels include divergent cytoplasmic N- and C-termini, and a characteristic 50-residue extracellular loop in the first homologous repeat. Deletion of the extracellular loop (Δ76–124) reduced the average current density in patches, increased spontaneous activity and generated a larger sub-population of high-conductance channels, while activation by tension augmented by arachidonic acid was fully retained. Further deletion of the C-terminal end (Δ76–124/Δ334–411) removed voltage dependency but otherwise produced no additional effect. In an attempt to generate a cysteine-free version of the channel, we mutated two remaining cysteines 159 and 219 in the transmembrane region. C219A did not compromise channel activity, whereas the C159A/S mutants were essentially inactive. Treatment with β-mercaptoethanol suggested that none of these cysteines form functionally-important disulfides.

Introduction

TREK-1, a two-pore (K_2P) background potassium channel[1] densely expressed in the CNS[2,3] is believed to be one of the key components mediating reactions to inflammatory signals in the brain.[4,5] The channel regulates resting potential in neurons and is believed to act as a hyperpolarizing (pacifying) neuroprotector in cases of ischemia, hypoxia, hyperthermia or swelling.[5-10] Hyperpolarizing TREK-1 activity has been directly implicated in the mechanisms of anesthesia by general volatile anesthetics[5,11] and in the setting of sensory thresholds for pain perception.[12] TREK-1 is reported to have an important role in the mood regulation.[13,14] TREK-1 was also proposed to play an essential role in determining membrane potential in embryonic atrial myocytes.[15] In patch-clamp setting, TREK-1 is perfectly mechanosensitive as it generates robust current transients in response to pressure pulses.[1,16] Besides its importance for the CNS function, TREK-1 channel is perhaps the most biophysically tractable membrane-bound target for arachidonic acid (AA), the major inflammatory intermediate, as well as for other lipid mediators.[17-19] The broad spectrum of activating stimuli[20] implies allostery and a high degree of interdomain coupling. The unusual tandem design of K2P channels (4TM, two-pore loops), distinct from 2TM (IR) and 6TM (K_V) K^+ channels, and the richness of functional information makes TREK-1 a good model of a 2P channel for biophysical and structural studies.

TREK-1 ($K_2P2.1$, KCNK2) belongs to the KCNK channel family with 15 mammalian members.[21] Like other two-pore K^+ channels, TREK-1 contains two homologous repeats, each having a KcsA-like 2TM topology, apparently a product of early gene duplication. As a result, TREK-1 is predicted to be a dimer,

*Correspondence to: Sergei Sukharev; Email: sukharev@umd.edu
Submitted: 07/29/10; Revised: 10/08/10; Accepted: 10/11/10
DOI: 10.4161/chan.5.1.13906

not tetramer, which may have important consequences for its regulation. Mouse and human TREK-1 proteins have alternative transcription initiation sites at M42 and M57, respectively,[22,23] which in these instances completely eliminate their cytoplasmic N-termini. Mouse TREK-1 has a 110-residue cytoplasmic C-tail with clusters of charged residues and three regulatory serine phosphorylation sites.[24] The cytoplasmic loop connecting the first and second repeats, a necessary component for the tandem organization, has a pattern of positive charges and can be modeled as a membrane-associated amphipathic helix (see accompanying manuscript), similar to the "slide" helix of inward rectifier KirBac1.1,[25,26] or to the predicted N-terminal helix of bacterial mechanosensitive channel MscL.[27,28] A distinct feature from other K^+ channels is a 50-residue extracellular loop (75–125) connecting the TM1 helix of the first homologous repeat (TM1a) with its P-loop. The functional role of the extracellular domain remains unclear.

The wealth of physiological information, however, emphasizes several missing links that could be addressed only by structural and biophysical studies. Currently, we do not have a crystal structure for any of the K_2P channels, and for this reason in the accompanying paper (Milac et al., pp. 23–33),[29] we describe the models for the resting, low-conductance and fully open states of the mouse TREK-1 channel built by homology on a KcsA template.[30] The homotetrameric KcsA structure with its free cytoplasmic N- and C-termini, however, could not be used directly to build a TREK-1 model, which had to incorporate the linker domain connecting two homologous repeats for which sequential differences preclude four-fold symmetry in the packing of the transmembrane helices. As a result, the resting state and the opening transition feature a two-fold symmetry, which probably has functional manifestations and physiological significance. One of the interesting possibilities is that the two-fold design may potentially permit allosteric regulation of the selectivity filter conformation by breaking and re-forming the pseudo four-fold symmetry of the K^+ coordinating groups. The model provides a large set of predictions that can then be tested with low-resolution techniques such as disulfide cross-linking, FRET and spin-labeling analysis.

In this paper we address the overall characteristics of the TREK-1 models as a prelude to analyzing finer details. On the assumption that TREK-1 is gated directly by tension transmitted through the lipid bilayer and thus the in-plane protein expansion confers the tension sensitivity,[31] we first compare the spatial scales of the conformational transition predicted by the model with the areal expansion deduced from the experimental dose-response curves. We then analyze functional characteristics of channels with deletions removing the parts that could not be accurately modeled due to the limitations of existing templates. Particularly, we demonstrate that neither the 50-residue extracellular loop connecting the first transmembrane helix with the pore domain nor the C-terminal domain beyond the residue 334 are essential for gating by membrane tension or AA. Finally, by eliminating two of the three endogenous cysteines and probing the functional state of the mutants we prepare the system for disulfide cross-linking analysis.

Results

TREK-1 homology model and the gating transition. The model of mouse TREK-1 built by homology to KcsA[29] is schematically represented in **Figure 1**. The model illustrates the impossibility of replicating the four-fold symmetrical KcsA-like design, where the pore is equally lined by four symmetrically arranged TM2s. The connector between **a** and **b** homologous repeats and a proline at a putative hinge region of TM2a prevent TM2a from packing the same way as TM2b with its free C termini. As a result, in the resting state, the constriction of the pore is formed mostly by two TM2b helices, whereas TM2a's embrace the core pair of tilted helices from the sides. The long extracellular loop (S75-H126) connecting TM1a with its pore helix is not included in the model since deletion of this loop does not preclude gating by tension or arachidonic acid (see below). The gate is occluded by a two-fold arrangement of A286, L289 and G293 residues on TM2b, whereas A175 on TM2a flank the gate from the side. The cytoplasmic connector between the **a** and **b** repeats has a pattern of 18-residue amphipathic helix with a number of positive charges that would interact with lipid headgroups. The part of the C-terminus included in the model (residues 308–333) was modeled as a coiled-coil bundle. The N-terminus was not included because it is difficult to predict without additional information and because it is absent with alternative transcription initiation at M42.

The transition is predicted to be a conical expansion of the cytoplasmic side of the protein associated with straightening of the kink between TM2a and the connector helix. In the open-state model, TM2a extends into the lipid, and probably beyond, which increases the footprint of the complex in the plane of the membrane. The area of the protein cross-section along the z (membrane normal) coordinate was calculated on the two models equilibrated in full-atom system with lipids. It indicates that the protein expands at the cytoplasmic side by 9 nm^2, whereas the extracellular side of the transmembrane barrel shrinks by about 4 nm^2 (**Fig. 1D**). Given that tension acts primarily at the boundaries between the hydrocarbon and the polar regions[32] roughly corresponding to the maxima of expansion and shrinking, the overall expansion is estimated to be about 5 nm^2. The modeled expansion of the cytoplasmic side of the pore at the same time creates an aqueous passage of ~12 Å in diameter permitting permeation of fully hydrated ions.

Experimental estimation of the spatial scale of protein expansion. We have expressed mouse TREK-1 in HEK-293T cells and obtained robust adaptive responses to pulses of negative pressure (**Fig. 2**). Using relatively large pipettes (~2 μm in diameter, BN 6–7) with bent tips oriented parallel to the focal plane we were able to reliably visualize patches under DIC optics and to determine their curvatures. Activation curves reconstructed from maximal current responses to progressively increasing stimuli combined with imaging revealed tension mid-points for TREK-1 activation as ~8.5 ± 1.1 mN/m in on-cell patches (cytoskeleton intact) and ~5.2 ± 0.4 mN/m in transparent blebs largely devoid of the cytoskeleton (n = 5 for each type). The experimental dependencies of the equilibrium constant Po/Pc were fitted to the Boltzmann

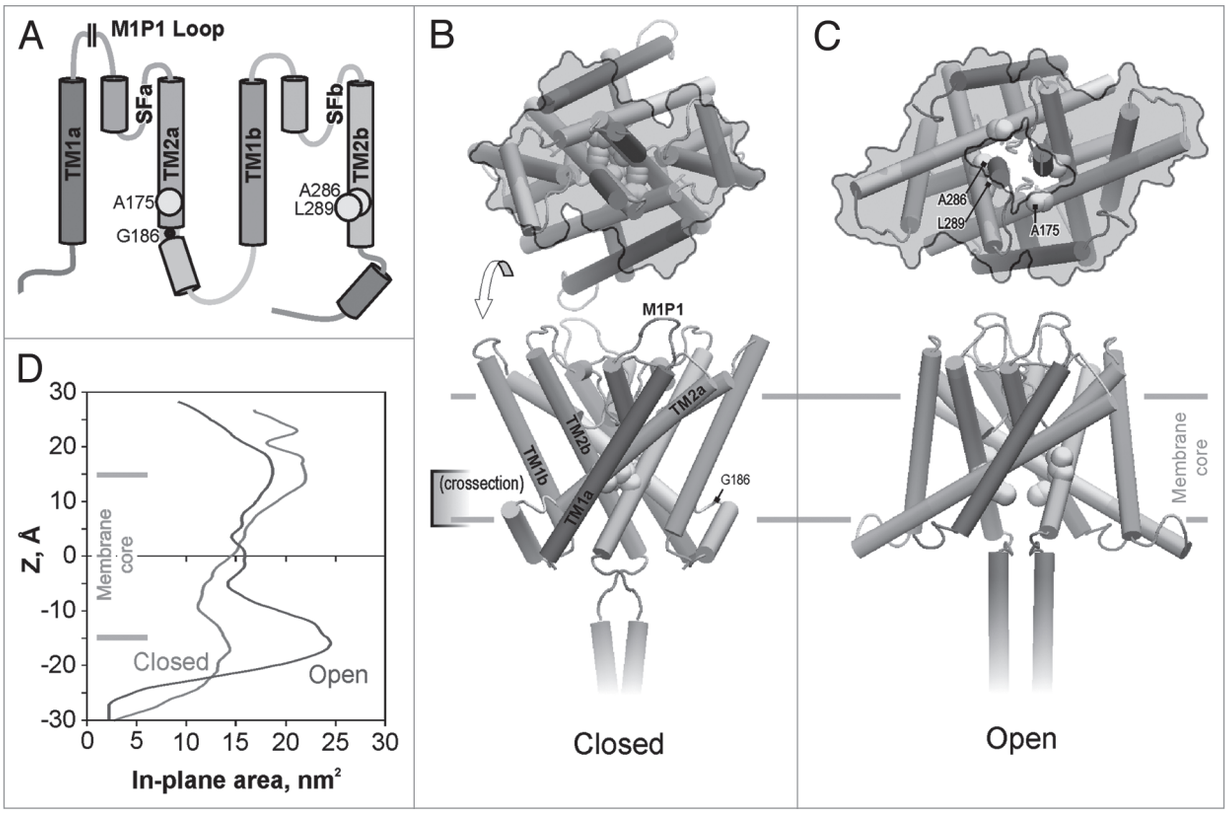

Figure 1. The topology of TREK-1 protein (A) and the structural models of the closed (B) and open (C) state built by homology to crystal structures of KcsA. The domains in the structures are color-coded as in the topology scheme (A); M1P1 designates the location of the extracellular 50-residue loop not included in the models. The yellow balls show the predicted positions of the hydrophobic residues forming the gate. G186 is the hinge glycine between the TM2a and the putative connector helix linking it to TM1b. In-plane expansion of the channel on opening (upper images on (B and C), as viewed from the cytoplasm) is illustrated by the gray contours marking the solvent-accessible channel surface for a slab between the levels of the gate (-5 Å) and the maximum tension on the cytoplasmic side (~-15 Å). Detailed in-plane area profiles along the z coordinate (D) estimate the total area change of the cytoplasmic part associated with the opening transition as ~5 nm^2. Color versions of our figures can be seen at http://www.landesbioscience.com/journals/channels/article/13906/

equation (see Methods). The maximal free energy differences between the states (ΔE) at zero tension and area changes (ΔA) associated with the transitions estimated from the two-dose-response curves (**Fig. 2**) were 7.8 kT and 3.7 nm^2 for the cell-attached patch and 3.9 kT and 3.9 nm^2 for the cytoskeleton-depleted bleb. Similar curves were obtained in four additional patches in each preparation and the averages of ΔE and ΔA were 6.6 ± 0.9 kT and 3.1 ± 0.4 nm^2 for cells and 4.0 ± 0.7 kT and 3.3 ± 0.6 nm^2 for blebs. The positive correlation between the ΔA and ΔE parameters in individual patches suggested that the channel population might be non-uniform and, as was shown previously,[33] even a slight spread of actual ΔE among individual channels in the population may lead to an underestimation of both ΔE and ΔA. For this reason, the maximal values observed represent patches with more uniform populations and provide values closer to real physical parameters. The maximal area parameters reflecting physical in-plane expansion of the protein in both cases are similar and close to the amount of protein expansion estimated from the model. The higher tension mid-point and estimated energy values for cell-attached patches suggest that the cortical cytoskeleton bears part of the tension applied to the patch. Similarly, treating cell-attached patches with cytoskeleton-disrupting agents such as colchicine and cytochalazin D were shown to augment mechano-activated currents of TREK-1 and TRAAK.[18,34]

Patch excision often removes desensitization. Figure 3 depicts a sequence of traces obtained in cell-attached configuration first and then upon patch pull-out and exposure to air. In the cell-attached configuration recorded in HEK-293T cells, TREK-1 desensitization was observed in 95% of the patches (n = 80). With large (BN 6–7) pipettes the decay time was generally slower than reported before,[16] likely due to patch membrane flow, which changes curvature over time.[35,36] Pulling the pipette out often leading to vesicle formation removed desensitization and slowed down the process of activation. Complete excision by brief exposure of the pipette tip to air increased the current, but in the majority of outcomes desensitization was absent. This suggests that either cytoskeleton or other intracellular components are required for desensitization. Both responses, before and after excision, were augmented by AA (not shown).

Effects of deletions on the functional responses of TREK-1 to membrane tension and AA. After deletion of the extracellular loop (Δ76–125) we observed WT-like mechano-activated currents

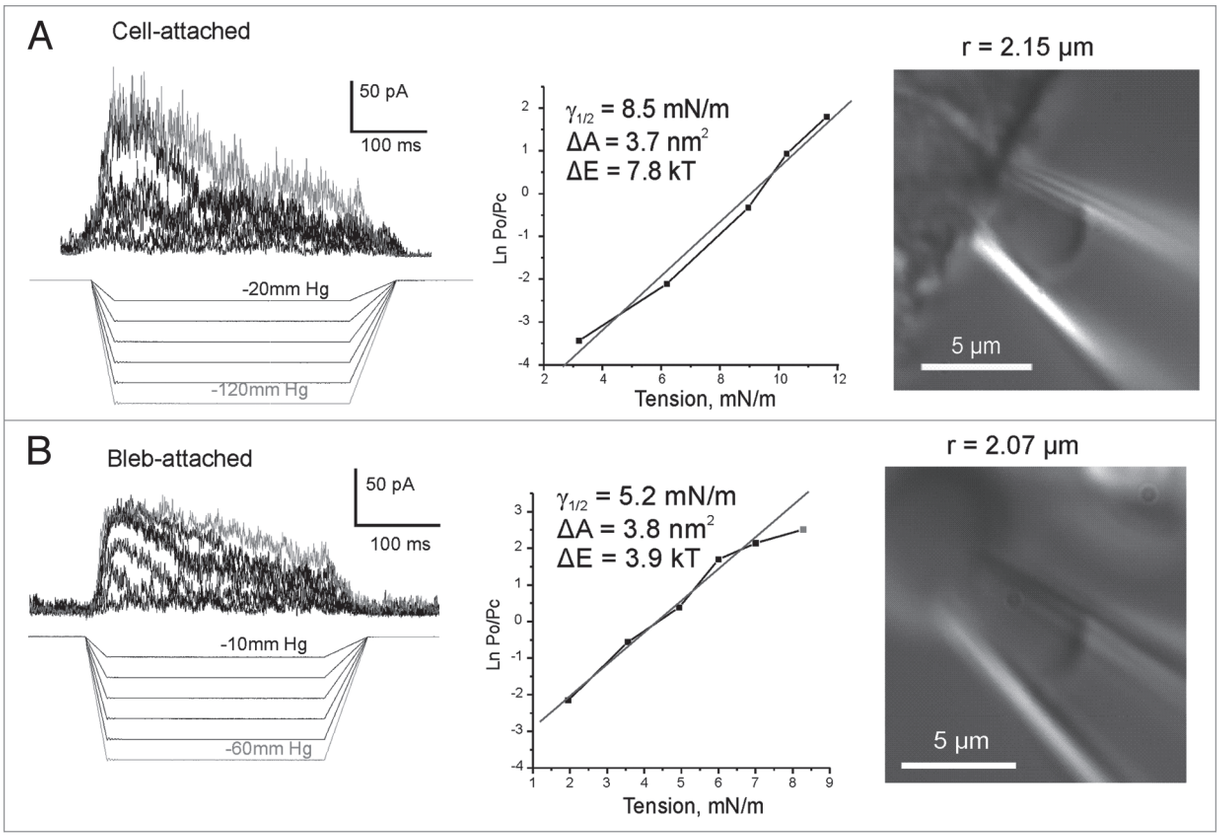

Figure 2. Dose-response curves obtained with patch imaging. TREK-1 activates in cytoskeleton-depleted blebs at considerably lower tensions than in regular cell-attached patches (HEK-293T cells). Imaging of patches was done in DIC with large-diameter (BN7) bent pipettes. Currents were recorded +40 mV in the pipette. The pressure protocols are depicted below the current traces. Fitting of the activation curves was done with the equation: $kT \cdot \ln(Po/Pc) = -\Delta E + \gamma \Delta A$, where Po and Pc are the probabilities of the channel finding in the open or closed states, ΔE is the free energy difference between the states, γ is tension, and ΔA is the area change associated with the transition. Color versions of our figures can be seen at http://www.landesbioscience.com/journals/channels/article/13906/

in the same range of pressures as those activating WT (**Fig. 4A**). With equal amount of DNA and similar level of transfection, as indicated by comparable fluorescence of independently expressed EGFP from the same plasmid, the maximal integral patch current of the Δ76–125 mutant was on average 10 times smaller compared to WT (**Table 1**). The current-to-voltage relationships recorded with voltage ramps (B) closely resembled that of WT.[37] While substantial fraction of channels remained functional, the decreased integral current could signify either a de-regulation or less efficient assembly/incorporation into the plasma membrane. A much higher occurrence of spontaneous activities observed at zero pressure (C) suggests that the channels are de-regulated. In wild-type, we observed tension-independent single-channel openings in 36% of patches (n = 40) that produced large mechano-activated currents. We saw spontaneous activities in 65% of patches from the Δ76–125 mutant (n = 130), generally producing smaller integral currents on saturating pressure steps. In both preparations, the fraction of patches with spontaneous activity was essentially independent on the recording configuration, cell-attached or excised. Besides higher presence of spontaneous openings in the deletion mutant, we also observed higher frequency of large-conductance "spiky" openings with the amplitude ~3 times larger than regular 50–60 pS conductance.[23] Previously, the high-conductance form was attributed to alternative initiation from internal Met codon that eliminates large part of the N-terminus, the behavior reported for both TREK-1,[22] and TREK-2,[38] channels. We did not eliminate the alternative translation initiation site M42, and thus cannot definitively evaluate relative contributions of the N-terminus and the extracellular loop in the switching to larger conductance. However, we can state that the absence of the loop either skews the distribution of transcripts toward the shorter form, or independently permits larger openings in the longer form. This interdependence needs to be analyzed in more detail.

Further truncation of the C-terminus (Δ76–125/Δ334–411) did not significantly alter the channel response to mechanical stimulation compared to the Δ76–125 mutant. Five to ten channels per patch (n = 15) were typically active under a 120 mm Hg pressure gradient (**Fig. 5A**); these channels with higher conductance and "spiky" appearance were as sensitive to tension as WT. We observed spontaneous activity (B) without pressure gradient comparable to that in the Δ76–125 mutant. We should be mindful about residual (background) stretch arising from the seal formation. The main difference that the C-terminal deletion

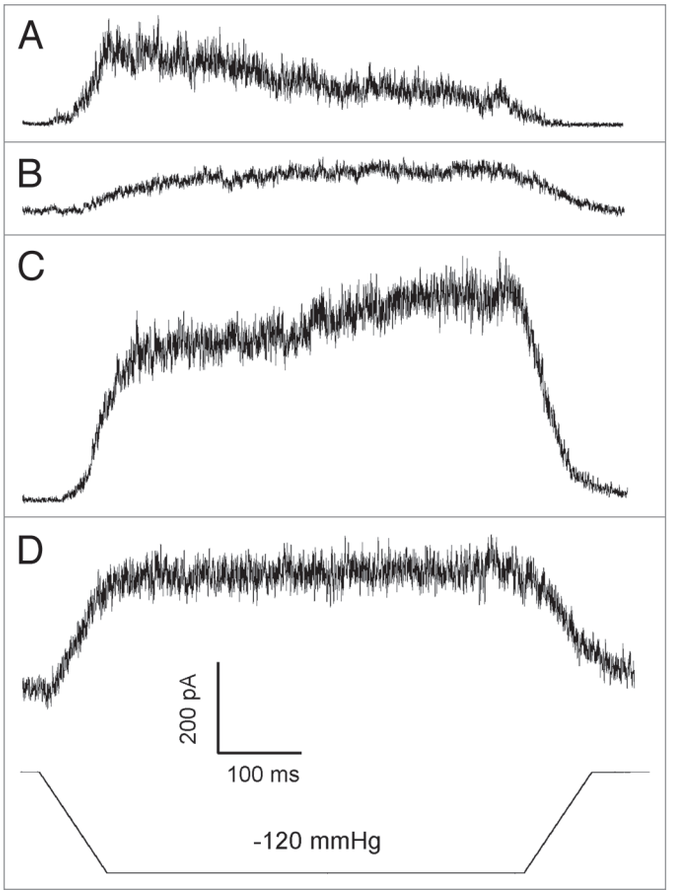

Figure 3. In more than 90% of the experiments desensitization was lost immediately after patch excision. The series of traces obtained in the same patch with the same pressure stimulus. Buffers: KCl (pipette)/NaCl (bath) Command voltage 40 mV. Pipette BN 5. (A) Cell-attached configuration (B) membrane vesicle blocks the tip (C) inside-out patch, immediately upon air exposure (D) inside-out patch, 5 minutes upon excision. The gradual current increase in (C) is likely due to flow of the membrane patch into the pipette, so more area and more channels were available. (D) Shows stabilization of the new patch position.

introduced was the absence of voltage-dependency of channel gating in response to a ±100 mV ramp of pressure. As previously, the response to the voltage ramp (**Fig. 5C**) was recorded under zero tension and the spontaneous activities were essentially voltage-independent, consistent with previous results.[37] This mutant remained fully sensitive to AA (**Fig. 5D**).

Cysteine 159 is essential. The functional state of the above truncation mutants makes it hopeful that the domain composition of the protein included in the model adequately represents functional channel. While the deletion of the extracellular loop removes one of the endogenous cysteines (C93), the Δ76–125/Δ334–411 TREK-1 still contains two of the endogenous cysteines (C159, C219), which may interfere with the future cross-linking assays. In our models C159 is located in the more extracellular portion of TM2a, where it interacts with the P segments of the selectivity filter, and C219 is near the central region of TM1b. In the first test we subjected WT TREK-1 channels to 10 mM β-mercaptoethanol from the pipette side and saw essentially no decrease in activity besides the regular time-dependent run-down (**Fig. 6A**). This experiment suggested that cysteines 159 and 219, which are ~15Å apart in our models, do not form functionally-important disulfides. We have replaced these cysteines with either serines of alanines and assayed the mutants for functionality. C159S and C159A were irresponsive to pressure gradients, but we found discernable TREK-1 activities in several patches exposed to arachidonic acid (**Fig. 6B**). C219A remained active, displaying spontaneous activities and a robust tension sensitivity. Activation of this mutant by stretch was also augmented by AA (data not shown). Therefore, only C159 appears to be essential for TREK-1 activation by stretch. If the activity of C159A/S mutant was absent at any circumstances, we might infer that this cysteine in the vicinity of the selectivity filer is somehow involved in protein folding in the endoplasmic reticulum or sorting in the Golgi, or that the mutations alter the structure of the selectivity filter to make it impermeant to ions. But the fact that arachidonic acid still invokes some activity is puzzling. If the C159A/S substitutions make the channel too "stiff" to be opened by tension, then arachidonic acid should be considered a stronger stimulus than membrane stretch.

Discussion

The absence of reliable structural information poses difficulties in interpreting rich functional phenomenology of TREK and precludes further mechanistic insight. In the accompanying paper (Milac, et al. pp. 23–33),[29] we presented models of the TREK-1 channel in the closed, low-conducting and open states built by homology to KcsA. The models provide a number of testable predictions, but here we presented only the "first layer" of phenomenology that supports the sufficiency of the domains included in our model for the processes of TREK-1 activation by stretch and arachidonic acid. Our major findings were that deletion of segments 76–125 and 334–411 not included in the model did not eliminate basic gating and selectivity properties of the TREK-1 channel. Thermodynamic analysis of the energetic and spatial scales of the transition predicts lateral expansion of the protein consistent with the model.

The gating process was modeled as a radial motion and tilting of TM2a and TM2b helices constrained by two-fold symmetry. The outward displacement and extension of the TM2 helices with the amphipathic linker domain was predicted to produce an approximately 5 nm^2 area expansion on the cytoplasmic side. The experimental analysis of activation curves generally supports this scale of conformational transition. The data obtained in cytoskeleton-depleted patches taken from blebs appear to provide more reliable thermodynamic parameters of gating transition ΔA = 3.7 nm^2 and ΔE = 3.9 kT. We should be cautious about the exact values, however, since heterogeneity of channels in the population tends to decrease the estimates.[33] Both the energy and in-plane expansion are much smaller in TREK-1 than in bacterial channels MscS or MscL.[33,39] Disruption of the cytoskeleton permits more channels to activate under a given pressure gradient suggesting that the channel senses tension in the membrane, while the cytoskeleton simply restrains membrane distension and does not participate in the conveying forces to the gate.[36,40]

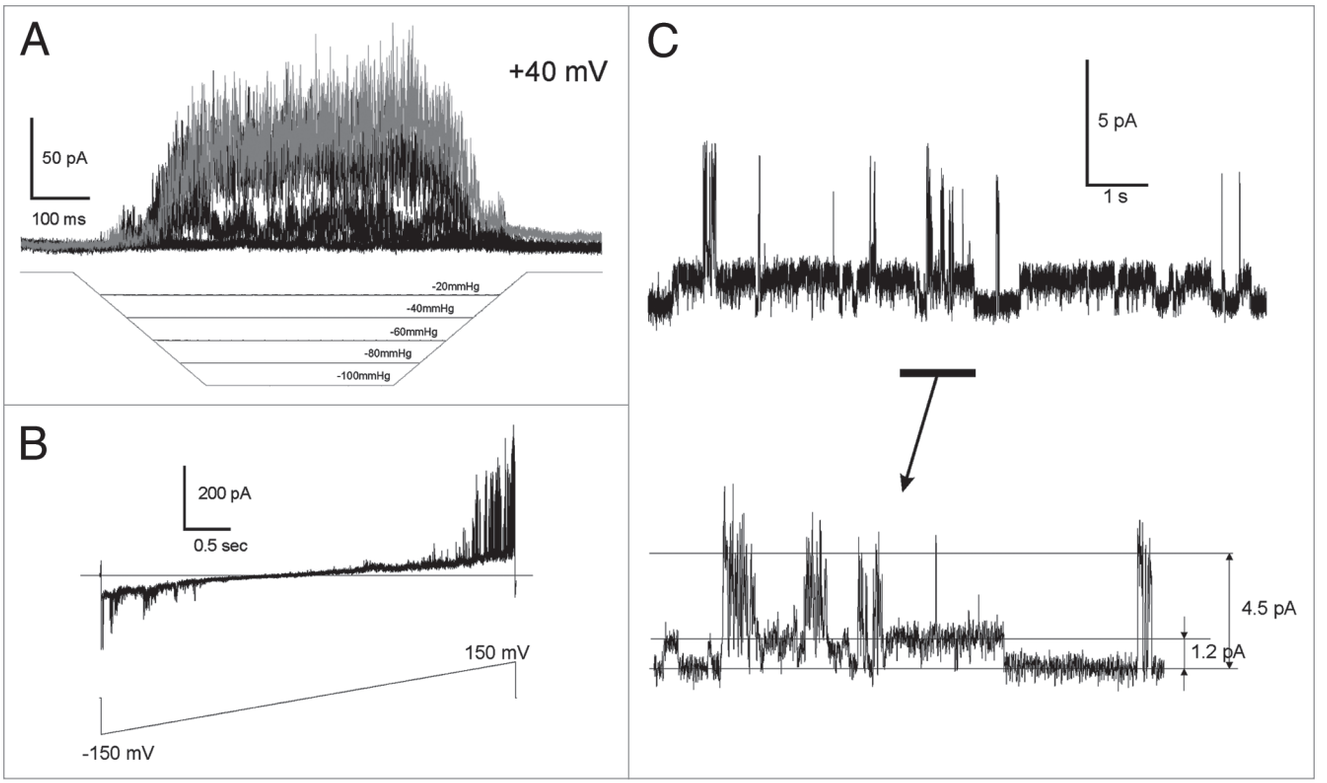

Figure 4. Deletion of the extracellular domain (loop) by re-closing S75 to H126 (Δ76–125) produces functional channels. (A) Activation by stretch in outside-out patch configuration (+40 mV pipette). (B) I–V curve recorded in cell-attached configuration with 155 mM KCl in the pipette and 150 NaCl, 5 KCl in the bath; the current reverses at V = -15 mV. (C) Spontaneous activity of Δ76–125 TREK-1 at zero pressure (excised patch). The single-channel traces show higher presence of larger conductance channels. Color versions of our figures can be seen at http://www.landesbioscience.com/journals/channels/article/13906/

Table 1. Peak currents obtained with WT and Δ76-125 TREK-1 in two recording configurations

	Cell-attached patches	Excised inside-out patches
WT	600 ± 370 pA, (n = 8)	520 ± 300 pA, (n = 9)
Δ76–125	55 ± 30 pA, (n = 10)	65 ± 40 pA (n = 6)
t-test	p < 0.002	p < 0.004

The currents were recorded under -40 mV command voltage in response to pressure pulses that patches could sustain with standard pipettes pulled to BN5.

Alternatively, some soluble cytoplasmic factors may affect the character of gating by interacting with the cytoplasmic N- and/or C-terminal domains. It remains to be determined whether tension in the lipid bilayer directly drives the transition, a task that would require purification and functional reconstitution of TREK-1. Patch excision in most of the cases led to the loss of desensitization suggesting the role of cytoplasmic factors in this process.

The models do not include several domains absent in the templates, and the purpose of the experiments presented in **Figures 4 and 5** was to test whether or not the missing domains are critical for the assembly and gating or merely serve as regulators/modulators that optimize the function. The N-terminal cytoplasmic domain is clearly dispensable since the alternatively initiated channel protein is functional and displays higher conductance.[22,38] Deletion of the extracellular loop connecting the TM1 helix of the first repeat with its pore helix in our experiments reduced functional expression, but 10% of channel activity remained (**Table 1**). Further deletion of the C-terminal domain did not produce a strong deleterious effect, but rather further de-regulated the channel by removing the voltage dependency[37] and increasing the spontaneous activity observed without applied pressure to the patch. We should be mindful, however, about residual tension in the patch due to gigaseal formation, which may serve as a weak but constantly present mechanical stimulus.[35]

The presented analysis put us one step closer to mechanistic understanding of mechanosensitivity of TREK-1 channel. It makes it hopeful that the model largely represents parts and domains that compose a functional but partially de-regulated TREK-1 channel. The Δ76–125/Δ334–411 TREK-1 still contains two of the endogenous cysteines (C159, C219), which may interfere with the cross-linking assays. Both C159S and C159A mutants were non-functional, however, C219A remained active. This additional mutation prepares the protein for future cross-linking trials. Fortunately C159 is near the extracellular surface where it would not be expected to interact with cysteines introduced into the inner gate region and cytoplasmic domain to test details of the proposed gating mechanisms.

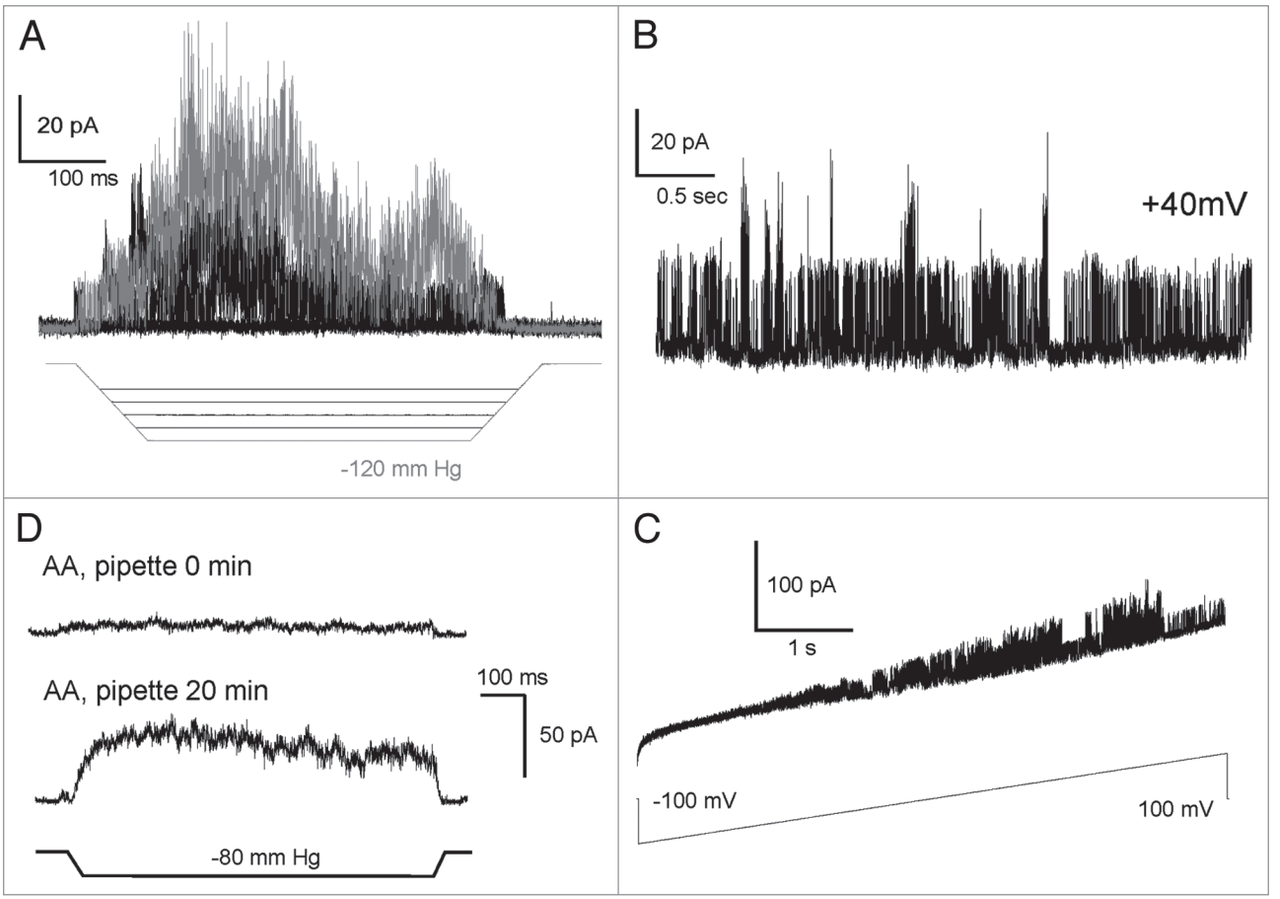

Figure 5. The responses of TREK-1 Δ76–125/Δ334–411 deletion mutant lacking both the extracellular loop and last 77 residues from the C-terminus. (A) Activation by pressure gradient. (B) Spontaneous activity at +40 mV. (C) Spontaneous activity in response to a ±100 mV voltage ramp. Deletion of the C-terminus removes voltage dependency. (D) Time-dependent effect of arachidonic acid (AA, 20 μm) added in the pipette, the upper trace was recorded immediately after seal formation and the bottom trace was recorded 20 min after. Without AA, the pressure stimulus invoked only a small current. Color versions of our figures can be seen at http://www.landesbioscience.com/journals/channels/article/13906/

Methods

Modeling. The modeling of TREK-1 was described in the accompanying paper (Milac et al., pp 23–33).[29] The models of the closed, low-conducting, and open states were subjected to two cycles of 15-ns unrestrained equilibration in lipids followed by 1-ns symmetry annealing utilizing the recently developed structure refinement protocol.[41] The effective cross-section areas of the protein along the membrane normal (z axis) were analyzed using a Tcl script custom-written for VMD.[42] Solvent-accessible surface was probed with a sphere of 1.4 Å radius. At every z level scanned with 0.5 Å steps, the cross-section area of the surface was estimated and the radius of a circle with equal area was considered to be an effective in-plane radius at that level. The expansion area defining the mechanosensitivity of TREK-1 was taken on the intracellular ("gate") half of the channel at the level of -17 to -15 Å where the maximum of the lateral tension/pressure profile is expected in POPC bilayer.[32]

Experimental procedures. The pIRES2-EGFP expression vector harboring mouse TREK-1 was kindly provided by Dr. Frederick Sachs (SUNY Buffalo). The following mutations TREK1 Δ76–125 (deletion of the extracellular loop), TREK-1 Δ76–125/Δ334–411 (deletions of the extracellular loop and C-terminus) TREK-1 Δ76–125/Δ334–411/C219A, TREK-1 Δ76–125/Δ334–411/C159A, TREK-1 Δ76–125/Δ334–411/C159S, TREK-1 Δ76–125/Δ334–411/C219A/C159A and TREK-1 Δ76–125/Δ334–411/C219A/C159S were sequentially generated using the Quick Change Kit (Stratagene).

WT TREK-1 and the mutants were expressed in HEK-293T cells by transfecting 0.1–0.3 μg DNA per 36 mm Petri dish using Lipofectamine 2000 (Invitrogen). Typically, about 50–60% of cells received the plasmid as judged by appearance of the separately expressed EGFP marker.

Pipettes were pulled out from borosilicate glass to bubble number (BN) of 5–7.[43] With sufficiently large pipettes, it was possible to visualize patches under differential interference contrast (DIC) optics with a 60x oil-immersion lens on an inverted Nikon Eclipse TE2000-S microscope. Images of patches captured with a camera were presented as spherical caps and their curvature was determined through fitting with NIS-Elements software (Nikon Instruments).

Recordings were done in either cell-attached or inside-out patches with the standard technique using Axopatch 200B,

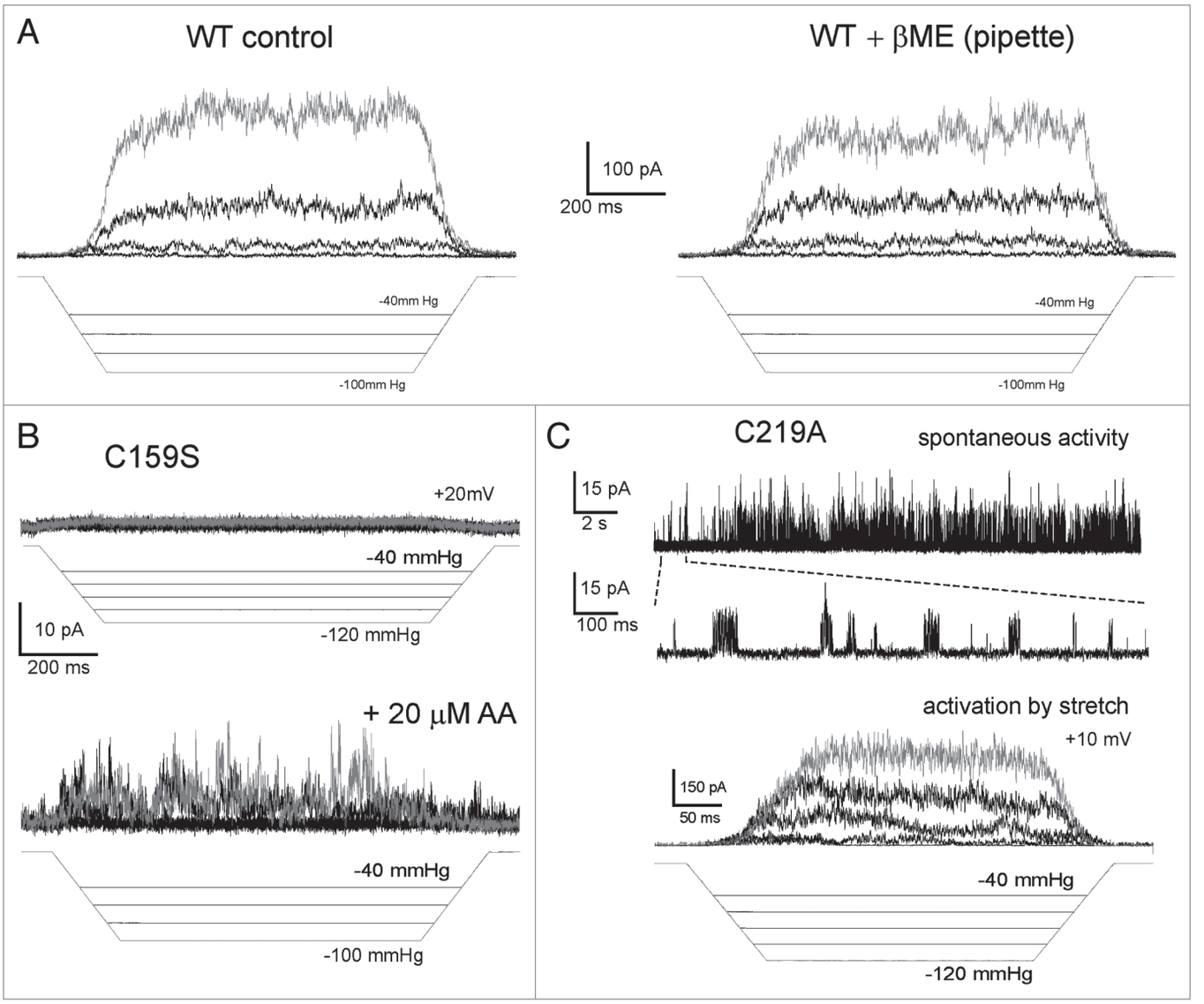

Figure 6. Elucidating the role of cysteines in TREK-1. (A) Mercaptoethanol (β-ME) present in the pipette shows no significant effect on activation of WT TREK-1 by pressure. (B) The C159S mutation introduced on the WT or Δ76–125/Δ334–411 background makes channel inactive under standard pressure protocol, but the mutants show small residual activity when the patch is pre-treated with AA. (C) C219A/Δ76–125/Δ334–411 mutant showed substantial spontaneous activity and was activated essentially as WT under standard pressure protocol. Color versions of our figures can be seen at http://www.landesbioscience.com/journals/channels/article/13906/

Digidata 1440 and PClamp 10 suite (Axon Instruments), signals were sampled at 20 kHz and filtered at 5 kHz. Typical buffer configuration was 155 mM KCl (pipette)/150 mM NaCl + 5 mM KCl (bath), 5 mM HEPES, pH 7.4. In some experiments beta-mercaptoethanol (5–10 mM in bath solution) was delivered to the chamber with a laboratory-built perfusion system.

Pre-programmed pressure pulses, ramps or trapezoid stimuli were delivered from an HSPC-1 pressure clamp machine (ALA Scientific Instruments). Transient peaks or steady population current in non-inactivating patches (I) were normalized to the amplitude at saturating pressure to obtain open probability. The energy (ΔE) and in-plane expansion (ΔA) parameters were extracted from dose-response curves fitted to a Boltzmann-type equation:

$$P_o/P_c = \exp[-(\Delta E - \gamma \Delta A)/kT]$$

where P_o and P_c are the open and closed probabilities, γ is membrane tension calculated from pressure gradient and patch curvature, k is Boltzmann constant and T is absolute temperature.

Acknowledgements

The authors thank Mrs. Naili Liu for technical assistance with cell cultures and DNA isolation. This work was supported in part by the Intramural Research Program of the National Institutes of Health, National Cancer Institute, Center for Cancer Research. The authors also thank Drs. Amanda Patel and Eric Honore (Centre National de la Recherche Scientifique) for discussions and intellectual support.

References

1. Patel AJ, Honore E, Maingret F, Lesage F, Fink M, Duprat F, et al. Mammalian two pore domain mechano-gated S-like K^+ channel. EMBO J 1998; 17:4283-90.
2. Hervieu GJ, Cluderay JE, Gray CW, Green PJ, Ranson JL, Randall AD, et al. Distribution and expression of TREK-1, a two-pore-domain potassium channel, in the adult rat CNS. Neuroscience 2001; 103:899-919.
3. Talley EM, Solorzano G, Lei Q, Kim D, Bayliss DA. Cns distribution of members of the two-pore-domain (KCNK) potassium channel family. J Neurosci 2001; 21:7491-505.
4. Buckler KJ, Honore E. The lipid-activated two-pore domain K^+ channel TREK-1 is resistant to hypoxia: implication for ischaemic neuroprotection. J Physiol 2005; 562:213-22.
5. Franks NP, Honore E. The TREK K2P channels and their role in general anaesthesia and neuroprotection. Trends Pharmacol Sci 2004; 25:601-8.
6. Maingret F, Patel AJ, Lesage F, Lazdunski M, Honore E. Mechano- or acid stimulation, two interactive modes of activation of the TREK-1 potassium channel. J Biol Chem 1999; 274:26691-6.
7. Caley AJ, Gruss M, Franks NP. The effects of hypoxia on the modulation of human TREK-1 potassium channels. J Physiol 2005; 562:205-12.
8. Maingret F, Lauritzen I, Patel AJ, Heurteaux C, Reyes R, Lesage F, et al. TREK-1 is a heat-activated background K^+ channel. EMBO J 2000; 19:2483-91.
9. Miller P, Peers C, Kemp PJ. Polymodal regulation of hTREK1 by pH, arachidonic acid and hypoxia: physiological impact in acidosis and alkalosis. Am J Physiol Cell Physiol 2004; 286:272-82.
10. Cohen A, Ben-Abu Y, Hen S, Zilberberg N. A novel mechanism for human K2P2.1 channel gating. Facilitation of C-type gating by protonation of extracellular histidine residues. J Biol Chem 2008; 283:19448-55.
11. Heurteaux C, Guy N, Laigle C, Blondeau N, Duprat F, Mazzuca M, et al. TREK-1, a K^+ channel involved in neuroprotection and general anesthesia. EMBO J 2004; 23:2684-95.
12. Alloui A, Zimmermann K, Mamet J, Duprat F, Noel J, Chemin J, et al. TREK-1, a K^+ channel involved in polymodal pain perception. EMBO J 2006; 25:2368-76.
13. Gordon JA, Hen R. TREKing toward new antidepressants. Nat Neurosci 2006; 9:1081-3.
14. Heurteaux C, Lucas G, Guy N, El YM, Thummler S, Peng XD, et al. Deletion of the background potassium channel TREK-1 results in a depression-resistant phenotype. Nat Neurosci 2006; 9:1134-41.
15. Zhang H, Shepherd N, Creazzo TL. Temperature-sensitive TREK currents contribute to setting the resting membrane potential in embryonic atrial myocytes. J Physiol 2008; 586:3645-56.
16. Honore E, Patel AJ, Chemin J, Suchyna T, Sachs F. Desensitization of mechano-gated K2P channels. Proc Natl Acad Sci USA 2006; 103:6859-64.
17. Chemin J, Patel A, Duprat F, Zanzouri M, Lazdunski M, Honore E. Lysophosphatidic acid-operated K^+ channels. J Biol Chem 2005; 280:4415-21.
18. Patel AJ, Lazdunski M, Honore E. Lipid and mechano-gated 2P domain K^+ channels. Curr Opin Cell Biol 2001; 13:422-8.
19. Maingret F, Patel AJ, Lesage F, Lazdunski M, Honore E. Lysophospholipids open the two-pore domain mechano-gated K^+ channels TREK-1 and TRAAK. J Biol Chem 2000; 275:10128-33.
20. Honore E. The neuronal background K2P channels: focus on TREK1. Nat Rev Neurosci 2007; 8:251-61.
21. Goldstein SA, Bayliss DA, Kim D, Lesage F, Plant LD, Rajan S. International Union of Pharmacology LV. Nomenclature and molecular relationships of two-P potassium channels. Pharmacol Rev 2005; 57:527-40.
22. Thomas D, Plant LD, Wilkens CM, McCrossan ZA, Goldstein SA. Alternative translation initiation in rat brain yields K2P2.1 potassium channels permeable to sodium. Neuron 2008; 58:859-70.
23. Honore E. Alternative translation initiation further increases the molecular and functional diversity of ion channels. J Physiol 2008; 586:5605-6.
24. Chemin J, Patel AJ, Duprat F, Lauritzen I, Lazdunski M, Honore E. A phospholipid sensor controls mechanogating of the K^+ channel TREK-1. EMBO J 2005; 24:44-53.
25. Kuo A, Gulbis JM, Antcliff JF, Rahman T, Lowe ED, Zimmer J. Crystal structure of the potassium channel KirBac1.1 in the closed state. Science 2003; 300:1922-6.
26. Enkvetchakul D, Jeliazkova I, Bhattacharyya J, Nichols CG. Control of inward rectifier K channel activity by lipid tethering of cytoplasmic domains. J Gen Physiol 2007; 130:329-34.
27. Steinbacher S, Bass R, Strop P, Rees DC. Structures of the prokaryotic mechanosensitive channels MscL and MscS. Mechanosensitive Ion Channels Part A 2007; 58:1-24.
28. Iscla I, Wray R, Blount P. On the structure of the N-terminal domain of the MscL channel: helical bundle or membrane interface. Biophys J 2008; 95:2283-91.
29. Milac AL, Anishkin A, Fatakia SN, Chow CC, Sukharev S, Guy HR. Structural models of TREK channels and their gating mechanism. Channels (Austin) 2011; 5:23-33
30. Zhou Y, Morais-Cabral JH, Kaufman A, MacKinnon R. Chemistry of ion coordination and hydration revealed by a K^+ channel-Fab complex at 2.0 A resolution. Nature 2001; 414:43-8.
31. Markin VS, Sachs F. Thermodynamics of mechanosensitivity. Phys Biol 2004; 1:110-24.
32. Gullingsrud J, Schulten K. Lipid bilayer pressure profiles and mechanosensitive channel gating. Biophys J 2004; 86:3496-509.
33. Chiang CS, Anishkin A, Sukharev S. Gating of the large mechanosensitive channel in situ: estimation of the spatial scale of the transition from channel population responses. Biophys J 2004; 86:2846-61.
34. Maingret F, Fosset M, Lesage F, Lazdunski M, Honore E. TRAAK is a mammalian neuronal mechano-gated K^+ channel. J Biol Chem 1999; 274:1381-7.
35. Suchyna TM, Markin VS, Sachs F. Biophysics and structure of the patch and the gigaseal. Biophys J 2009; 97:738-47.
36. Suchyna TM, Besch SR, Sachs F. Dynamic regulation of mechanosensitive channels: capacitance used to monitor patch tension in real time. Phys Biol 2004; 1:1-18.
37. Maingret F, Honore E, Lazdunski M, Patel AJ. Molecular basis of the voltage-dependent gating of TREK-1, a mechano-sensitive K^+ channel. Biochem Biophys Res Commun 2002; 292:339-46.
38. Simkin D, Cavanaugh EJ, Kim D. Control of the single channel conductance of K2P10.1 (TREK-2) by the amino-terminus: role of alternative translation initiation. J Physiol 2008; 586:5651-63.
39. Akitake B, Anishkin A, Sukharev S. The "dashpot" mechanism of stretch-dependent gating in MscS. J Gen Physiol 2005; 125:143-54.
40. Zhang Y, Gao F, Popov VL, Wen JW, Hamill OP. Mechanically gated channel activity in cytoskeleton-deficient plasma membrane blebs and vesicles from Xenopus oocytes. J Physiol 2000; 523:117-30.
41. Anishkin A, Milac AL, Guy HR. Symmetry-restrained molecular dynamics simulations improve homology models of potassium channels. Proteins 2010; 78:932-49.
42. Humphrey W, Dalke A, Schulten K. VMD: visual molecular dynamics. J Mol Graph 1996; 14:33-8.
43. Mittman S, Flaming DG, Copenhagen DR, Belgum JH. Bubble pressure measurement of micropipet tip outer diameter. J Neurosci Methods 1987; 22:161-6.